Electropolymerization of Pd(II) Complexes Containing Phosphinoterthiophene Ligands

Olivier Clot, Michael O. Wolf,* and Brian O. Patrick

Contribution from the Department of Chemistry, The University of British Columbia, Vancouver, British Columbia V6T 1Z1, Canada

Received June 20, 2001

Abstract: A series of Pd complexes of 3′-diphenylphosphino-2,2′:5′2″-terthiophene (**1a**, dppterth) in which the metal is coordinated in three different modes have been prepared and electropolymerized, resulting in the formation of conductive thin films. In $[Pd_2(\mu\text{-}Cl_2)$(dppterth-$P,C^3)_2]$ (**3a**) the metal is P,C-coordinated, in $[PdCl_2$-(dppterth-$P)_2]$ (**4a**) the coordination is monodentate via the phosphine, and in [Pd(dppterth-P,C^3)(dppterth-P,S^1)][PF_6] (**5a**) both P,C- and P,S-coordination modes are found. In **5a**, the coordinated thiophene is hemilabile and may be displaced by reaction with more strongly coordinating ligands such as isocyanides. To probe the effect of blocking the α-position of the terthienyl moiety with methyl groups, 3′-diphenylphosphino-5-methyl-2,2′:5′2″-terthiophene (**1b**, Me-dppterth) and 3′-diphenylphosphino-5,5″-dimethyl-2,2′:5′2″-terthiophene (**1c**, Me_2-dppterth) were prepared, and the corresponding series of Pd complexes was synthesized. One of these complexes, [Pd(Me_2-dppterth-P,C^3)(Me_2-dppterth-P,S^1)][PF_6] (**5c**), has been crystallographically characterized. The electropolymerized films prepared from **5a** react with isonitriles, and shifts in the absorption spectra of the electropolymerized materials are observed upon reaction. A Pd complex has also been prepared from 5-diphenylphosphino-2,2′:5′2″-terthiophene (**2**, 5dppterth), and this complex has been electropolymerized. All the electropolymerized thin films have been characterized using EDX analysis, which demonstrates good correspondence with the elemental analysis of the respective monomers, and the maximum conductivities of the films are near 10^{-4} S cm^{-1}. Comparing the electropolymerization behavior of the complexes, along with their electrochemical and spectroscopic data, allows conclusions to be drawn regarding the involvement of π-delocalization and the metal group in the conductivity of the materials.

Introduction

Materials with π-conjugated backbones are being intensively studied because of their interesting electronic and optical properties, which include high conductivities, electroluminescence, and photochromism.[1] π-Conjugated materials which incorporate transition metals are of significance, because the metal has the capacity to influence the overall properties of these materials, possibly giving rise to unprecedented or enhanced properties.[2,3] A wide range of possible applications is being explored for these materials, including applications as photorefractive materials,[4] as chemosensory materials,[5,6] and in electroluminescent devices.[7] In all of these applications, the nature of the electronic interaction between the metal and the conjugated backbone is of central importance, and this is influenced by the bonding between the metal and the backbone. The metal may be strongly electronically coupled by direct coordination to (or insertion in) the backbone, while weaker coupling results when a saturated linker is present. Functional materials based on conjugated frameworks in which the reactivity of the metal center may be tuned by using the redox characteristics of the backbone have also been explored.[8,9]

Our own efforts have focused on metal-containing hybrid materials in which the π-backbone is an oligo- or polythiophene,[10−12] principally because thiophene-based materials are readily synthetically accessible, relatively stable, and may be polymerized via electrochemical routes. A structural motif which has been less explored involves the metal center linking conjugated chains leading to cross-linked networks; in this case, the metal may be involved in charge transport through the bulk material. Weder and co-workers recently demonstrated such a hybrid material in which Pt centers bridge poly(*p*-phenylene ethynylene) chains, resulting in changes in the photophysical behavior of the polymer.[13] In a recent Communication, we reported the first example of a polythiophene derivative in which conjugated chains are linked by Pd bridges in which the metal is σ-bonded to a C of the backbone.[14] Here, we further explore

* To whom correspondence should be addressed. E-mail: mwolf@chem.ubc.ca. Fax: 604-822-2847.

(1) Skotheim, T. A.; Elsenbaumer, R. L.; Reynolds, J. R. *Handbook of Conducting Polymers*, 2nd ed.; Marcel Dekker: New York, 1998.
(2) Kingsborough, R. P.; Swager, T. M. *Prog. Inorg. Chem.* **1999**, *48*, 123−231.
(3) Wolf, M. O. *Adv. Mater.* **2001**, *13*, 545−553.
(4) Peng, Z.; Yu, L. *J. Am. Chem. Soc.* **1996**, *118*, 3777−3778.
(5) Zhu, S. S.; Carroll, P. J.; Swager, T. M. *J. Am. Chem. Soc.* **1996**, *118*, 8713−8714.
(6) Zhu, S. S.; Swager, T. M. *J. Am. Chem. Soc.* **1997**, *119*, 12568−12577.
(7) Wong, C. T.; Chan, W. K. *Adv. Mater.* **1999**, *11*, 455−459.
(8) Weinberger, D. A.; Higgins, T. B.; Mirkin, C. A.; Liable-Sands, L. M.; Rheingold, A. L. *Angew. Chem., Int. Ed. Engl.* **1999**, *38*, 2565−2568.
(9) Weinberger, D. A.; Higgins, T. B.; Mirkin, C. A.; Stern, C. L.; Liable-Sands, L. M.; Rheingold, A. L. *J. Am. Chem. Soc.* **2001**, *123*, 2503−2516.
(10) Zhu, Y.; Millet, D. B.; Wolf, M. O.; Rettig, S. J. *Organometallics* **1999**, *18*, 1930−1938.
(11) Zhu, Y.; Wolf, M. O. *Chem. Mater.* **1999**, *11*, 2995−3001.
(12) Clot, O.; Wolf, M. O.; Yap, G. P. A.; Patrick, B. O. *J. Chem. Soc., Dalton Trans.* **2000**, 2729−2737.
(13) Huber, C.; Bangerter, F.; Caseri, W. R.; Weder, C. *J. Am. Chem. Soc.* **2001**, *123*, 3857−3863.

10.1021/ja016465m CCC: $20.00
Published on Web 09/25/2001

Scheme 1

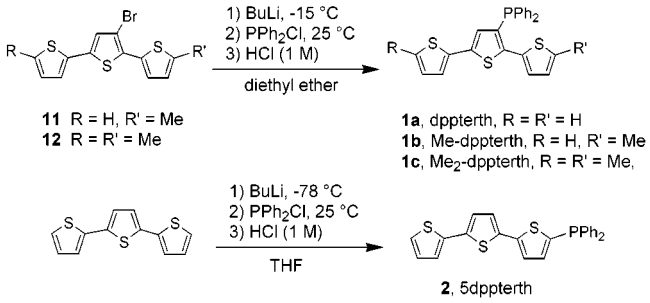

the materials formed by electropolymerization of Pd(II) complexes containing phosphinoterthiophene ligands exhibiting several different bonding modes. This gives insight into structural control and electronic interactions in such cross-linked materials.

Results

Syntheses and Structures of Ligands and Complexes. The phosphinoterthiophene ligand 3′-diphenylphosphino-2,2′:5′2″-terthiophene (**1a**, dppterth)[12] has been previously reported. The related mono- and dimethyl terminated derivatives of dppterth (**1b** and **1c**) have been prepared in an attempt to address questions related to the electropolymerization of metal complexes containing these ligands (vide infra). Compounds **1b** (Me-dppterth) and **1c** (Me_2-dppterth) were synthesized by the reaction of 3′-bromo-5-methyl-2,2′:5′2″-terthiophene (**11**) and 3′-bromo-5,5′-dimethyl-2,2′:5′2″-terthiophene (**12**), respectively, with *n*-butyllithium at −15 °C followed by reaction with PPh_2Cl at room temperature (Scheme 1). Compounds **1b** and **1c** were isolated as bright yellow powders, which oxidized slowly in air. The structurally allied compound 5-diphenylphosphino-2,2′:5′2″-terthiophene (**2**, 5dppterth) which is expected to bind in a monodentate fashion via the terminal phosphine has been prepared using a similar procedure.

The products obtained from the reactions of **1a**−**c** with $PdCl_2$ are dependent on the amount of metal halide used in the reaction. Complexes **3a**−**c** were synthesized via the reactions of **1a**−**c** in ethanol/acetonitrile solution with a small excess of $PdCl_2$ in water (Scheme 2). Upon addition of the phosphine to the solution of $PdCl_2$, the products **3a**−**c** immediately precipitated and were collected by filtration as yellow-orange, air-stable powders.

The structures of **3b**,**c** were assigned by comparison of their NMR spectra with those of **3a**, whose solid-state structure was reported previously.[14] Because all three ligands **1a**−**c** are closely related, we assign the geometry of **3b**,**c** to dimetallic complexes in which the Pd centers are in a square planar environment with bridging chlorides and the phosphinoterthiophene ligands bound via the phosphine and C3 of the terthienyl group. If an excess of **1a** dissolved in ethanol is added to $PdCl_2$ in water/ethanol solution cooled to 0 °C, cyclopalladation does not take place, and the resulting products are exclusively **4a** and unreacted $PdCl_2$, with no **3a** detected by NMR.

Complex **3a** was shown previously to react with phosphines and isocyanides to give mononuclear complexes via cleavage of the dichloro bridge.[14] Similarly, the dichloro bridge in **3b** can also be cleaved, and the reaction with tolyl isocyanide yields complex **7b** in which the isocyanide binds in a terminal fashion to Pd (ν_{NC} = 2193 cm^{-1} in chloroform). In **7b**, the isocyanide is most likely cis to the σ-bonded carbon, as is typically the case in related compounds.[15]

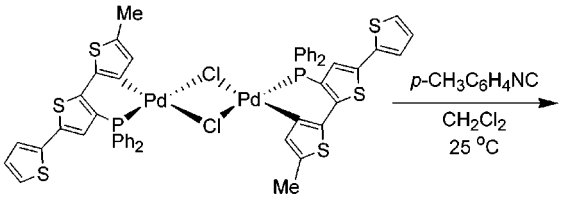

3b

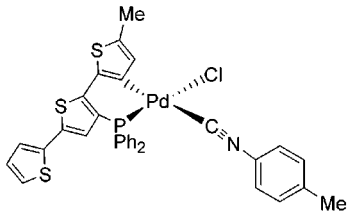

7b

When $PdCl_2$ in water is added to an excess of the appropriate phosphinoterthiophene ligand in ethanol at 50 °C, complexes **4a**−**c** and **6** are obtained in good yield (Scheme 2). These complexes are not soluble in the solvent mixture and rapidly precipitate out of the solution as yellow, air-stable solids during the reaction. The ^{31}P NMR spectra of all four complexes contain only one singlet at $\sim\delta_P$ 10, indicating that the phosphines are equivalent, and elemental analyses are consistent with the general formula [$PdCl_2$(phosphinoterthiophene)$_2$]. The far-IR spectrum of complex **4a** contains a strong band at 357 cm^{-1} corresponding to the Pd−Cl stretch, indicating that the chlorines are trans and resulting in an all-trans square planar geometry common to many Pd bis(phosphine) complexes.[16,17] The spectroscopic data for compounds **4b**,**c** and **6** indicate that these have analogous structures to **4a**.

Chloride abstraction from bis(phosphine) complexes **4a**−**c** using 2 equiv of $AgBF_4$, followed by metathesis with NH_4PF_6, results in formation of monocationic complexes **5a**−**c** in good yield (Scheme 2). All three complexes were isolated as orange, air-stable powders. Although attempts to grow crystals of **5a** were unsuccessful, small platelet-like crystals of **5c** were grown from a chloroform/diethyl ether mixture, and the solid-state structure was established by X-ray crystallography. The structure is shown in Figure 1, and selected bond lengths and angles are collected in Table 1. The two Me_2-dppterth ligands bind differently to the Pd; one ligand coordinates via a P,C mode resulting in a six-membered ring with a P−Pd−C bite angle of 80.4(3)°. The second ligand coordinates in a P,S mode with the sulfur coordinated in an η^1 fashion via the terminal thiophene ring, resulting in a six-membered ring with a P−Pd−S bite angle of 84.96(9)°. The complex is distorted from planarity toward a tetragonal geometry (S−Pd−C = 168.4(3)° and P−Pd−P = 163.56(9)°).

A number of species have been reported containing a bond or interaction between palladium and the sulfur of a thiophene ring;[18−26] however, only two of these have been structurally characterized.[25,26] In [Pd(SDPDTP)]Cl (SDPDTP = 5,20-

(14) Clot, O.; Wolf, M. O.; Patrick, B. O. *J. Am. Chem. Soc.* **2000**, *122*, 10456−10457.

(15) Hayashi, Y.; Isobe, K.; Nakamura, Y.; Okeya, S. *J. Organomet. Chem.* **1986**, *310*, 127−134.

(16) *Comprehensive Organometallic Chemistry: the Synthesis, Reactions and Structures of Organometallic Compounds*; Wilkinson, G., Ed.; Pergamon: Oxford, 1982; Vol. 6.

(17) *Comprehensive Organometallic Chemistry II: A Review of the Literature 1982−1994*; Abel, E. W., Stone, G. A., Wilkinson, G., Eds.; Pergamon: Oxford, 1995; Vol. 9.

Scheme 2

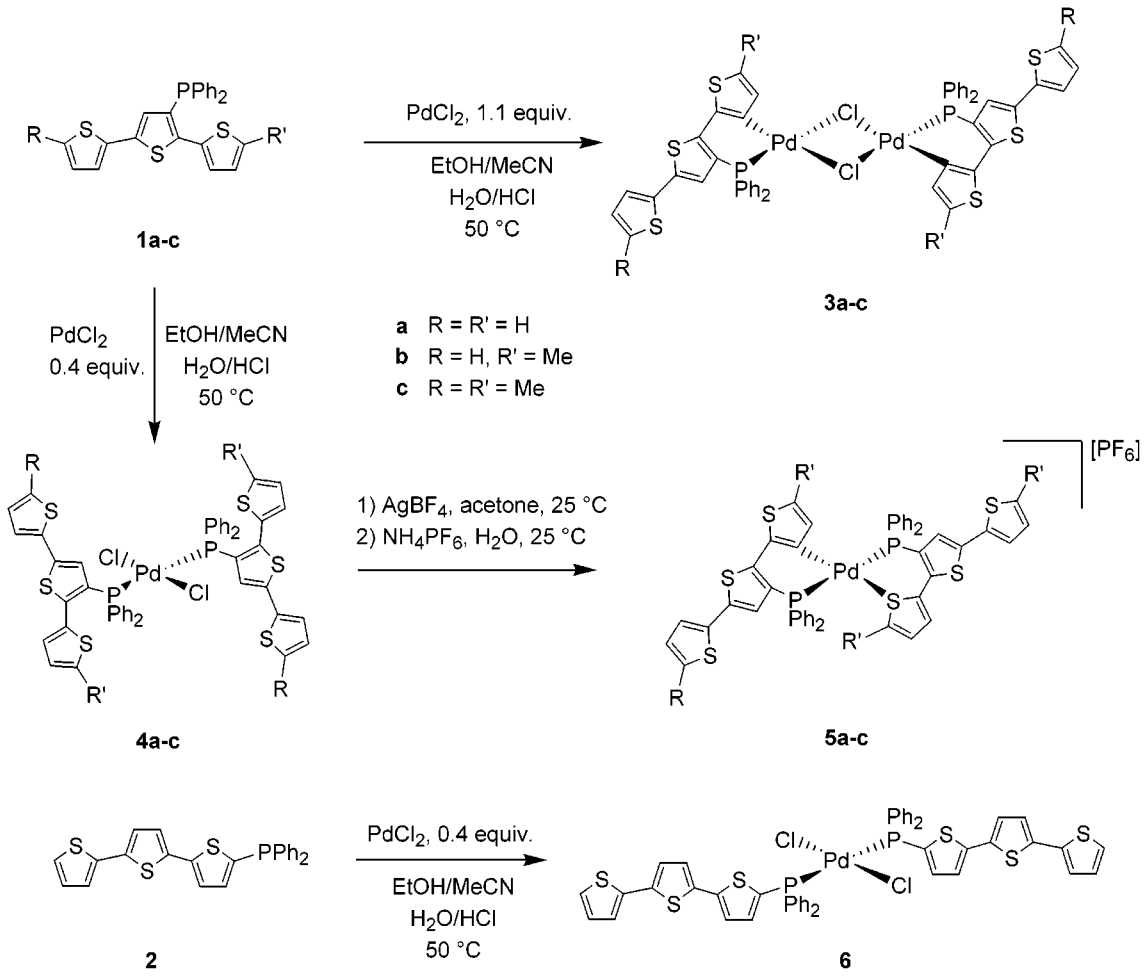

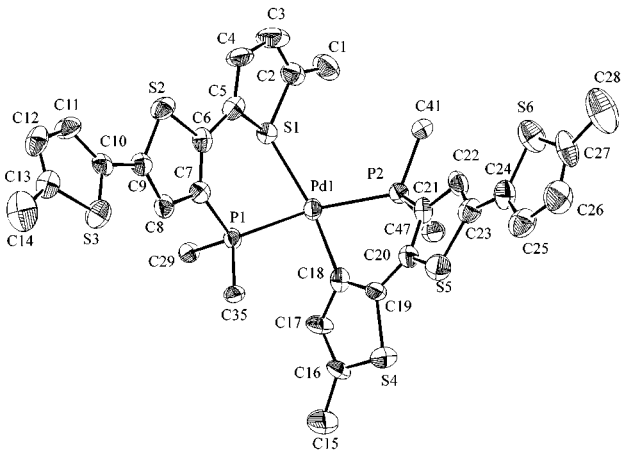

Figure 1. X-ray crystal structure of **5c**. The hydrogen atoms, phenyl groups, and PF_6 anion are omitted for clarity. Thermal ellipsoids are drawn at 30% probability.

Table 1. Selected Bond Lengths and Angles for **5c**

Bond Length, Å			
Pd(1)−S(1)	2.427(3)	Pd(1)−C(18)	2.01(1)
Pd(1)−P(1)	2.352(2)	Pd(1)−P(2)	2.307(3)
S(1)−C(2)	1.74(1)	S(4)−C(16)	1.73(1)
S(1)−C(5)	1.745(9)	S(4)−C(19)	1.76(1)
C(2)−C(3)	1.34(2)	C(16)−C(17)	1.37(1)
C(3)−C(4)	1.41(2)	C(17)−C(18)	1.41(1)
C(4)−C(5)	1.34(1)	C(18)−C(19)	1.39(1)

Bond Angle, deg			
S(1)−Pd(1)−C(18)	168.4(3)	P(1)−Pd(1)−P(2)	163.56(9)
S(1)−Pd(1)−P(1)	84.96(9)	S(1)−Pd(1)−P(2)	108.2(1)
P(1)−Pd(1)−C(18)	88.1(3)	P(2)−Pd(1)−C(18)	80.4(3)
Pd(1)−P(1)−C(7)	112.5(3)	Pd(1)−P(2)−C(21)	103.9(3)
Pd(1)−P(1)−C(29)	113.2(3)	Pd(1)−P(2)−C(41)	121.0(3)
Pd(1)−P(1)−C(35)	115.0(3)	Pd(1)−P(2)−C(47)	116.0(3)
C(2)−S(1)−C(5)	92.8(5)	C(16)−S(4)−C(19)	92.5(5)
S(1)−C(2)−C(3)	109.3(8)	S(4)−C(16)−C(17)	109.7(8)
S(1)−C(5)−C(4)	108.3(8)	S(4)−C(19)−C(18)	110.5(8)
C(2)−C(3)−C(4)	114(1)	C(16)−C(17)−C(18)	116(1)
C(3)−C(4)−C(5)	115(1)	C(17)−C(18)−C(19)	111(1)

diphenyl-10,15-ditolyl-21-thiaporphyrin),[26] the Pd−S bond length (2.208(5) Å) is shorter than the corresponding bond in **5c** and shorter than the sum of the covalent radii of Pd and S (2.35 Å).[27] On the other hand, in $[Pd(\mu\text{-}C_3H_5)(L)][CF_3SO_3]$ (L = 2,5,8-trithia[9](2,5)thiophenophane),[25] the Pd−S (thiophene) distance (2.786(4) Å) is much longer than both the Pd−S bond in **5c** and the sum of the covalent radii; however, because the Pd−S distance is shorter than the sum of the van der Waals radii (3.4 Å),[28] an apical Pd−S bond was postulated.[25] Many of the metal−thiophene sulfur bonds reported in the literature are near or slightly longer than the sum of the covalent radii,[12,25,29−40] and this is also the case for **5c** where the Pd−S

(18) Russell, M. J. H.; White, C.; Yates, A.; Maitlis, P. M. *J. Chem. Soc., Dalton Trans.* **1978**, 857−861.
(19) Larock, R. C.; Leach, D. R.; Bjorge, S. M. *Tetrahedon Lett.* **1982**, *23*, 715−718.
(20) Athar, M.; Ahmed, N. *Indian J. Chem., Sect. A* **1983**, *22A*, 1055−1057.
(21) Joginadham, C.; Bhagwat, U. A.; Mukhedkar, V. A.; Mukhedkar, A. J. *Indian J. Chem., Sect. A* **1987**, *26A*, 341−344.

distance is 2.427(3) Å. The thiophene ring plane has a tilt angle of 141° with respect to the Pd−S bond, which is within the range typically observed for η^1-S thiophene bound to various metals.[12,41−43] The rather large value of the tilt angle suggests that there is significant back-bonding to the thiophene.[44]

The bond lengths and angles of the sulfur-coordinated thiophene in **5c** differ from the analogous values in thiophene.[45] The coordinated ring is distorted in a fashion similar to that of the coordinated thiophenes in ruthenium complexes in which dppterth is chelated in a P,S fashion with longer C−S and shorter C═C bonds than in thiophene.[12] Similar distortions have also been observed in other metal−thiophene complexes and are believed to be due to a slight loss of aromaticity in the ring upon coordination.[46] In compound **5c**, it is also possible to compare within the same complex the relative distortions imposed on the terthienyl moieties by the P,C- and P,S-coordination modes. Most of the bond lengths and angles within the two terthienyl moieties are comparable, except for those in the terminal ring that is coordinated to the metal. The deformations in the C-coordinated thiophene are larger than those in the S-coordinated ring, indicating that coordination of thiophene to palladium via the sulfur is less disruptive to the aromaticity than the formation of a metal−carbon σ-bond between Pd and thiophene.

The ^{31}P NMR spectra of **5a**−**c** all contain two pairs of doublets due to the phosphines, indicating the presence of a mixture of two products in solution, as well as a septet corresponding to the PF_6 anion (Figure 2). The pair of doublets with the larger J_{PP} corresponds to the complex in which the phosphines are trans while the other pair is due to a cis orientation of the phosphines. The structures of **5a**,**b** were established to be analogous to that of **5c** with one of the ligands P,S-coordinated via the terminal thiophene bound η^1(S) and the other ligand chelating P,C via the C3 of the terthienyl moiety, by comparing their NMR spectra with that of **5c**.

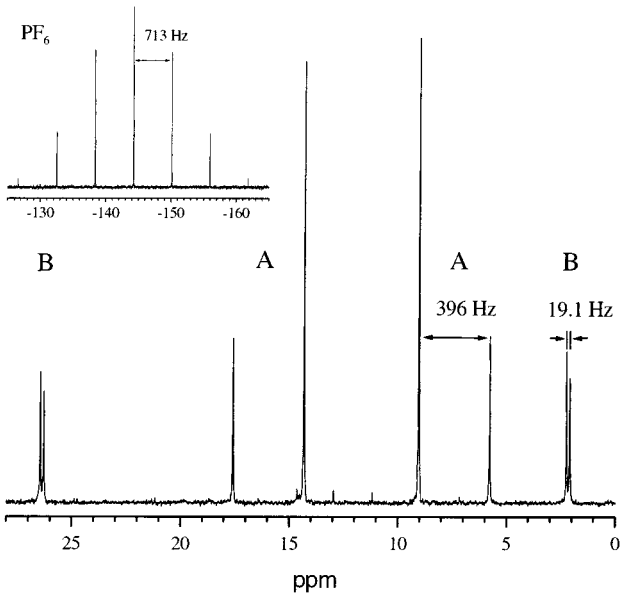

Figure 2. ^{31}P NMR spectrum of **5b** in $CDCl_3$ showing a mixture of (A) *trans*- and (B) *cis*-[Pd(Me-dppterth-*P*,*C*^{3})(Me-dppterth-*P*,*S*^{1})][PF_6].

The cis/trans ratios of **5a**−**c** are solvent dependent. Solutions of **5c** contain ∼30% of the cis compound in $CDCl_3$, ∼50% in acetone-d_6, and near 0% in MeOH-d_4 (ratios determined by NMR). For compounds **5a**,**b**, the cis/trans ratios in solution are ∼6% cis for **5a** and ∼34% cis for **5b** (in $CDCl_3$, determined by NMR). Cis−trans isomerization in these complexes may occur via two different pathways: either via a trigonal intermediate by dissociation of the coordinated thiophene ring or via a nondissociative pathway, involving a tetragonal intermediate in which the two dppterth ligands remain chelated to Pd. Dissociative pathways are generally promoted by the presence of coordinating solvents such as MeOH. However, no evidence of coordination of MeOH was detected in the ^{31}P NMR spectrum of **5c** in $CDCl_3$ when a large excess (∼10 000 equiv) of MeOH was added, and virtually no cis isomer was detected by NMR in MeOH-d_4. Because in the solid state **5c** has a pseudotetrahedral structure, and complexes such as [$NiBr_2(PPh_2Me)_2$] are known to isomerize between square planar and tetrahedral geometries,[47] the nondissociative pathway is more likely to be involved in the cis−trans isomerization of **5a**−**c**.

In complexes **5a**−**c**, the dppterth ligand that is P,S-coordinated is hemilabile. For example, when **5a** reacts with tolyl isocyanide in methylene chloride at 25 °C, the resulting product **8a** shows a new IR band at 2194 cm^{-1}, characteristic of a C-coordinated N≡C group. The ^{31}P NMR spectrum of **8a** contains a doublets of doublets (J_{PP} = 388 Hz) similar to that obtained for trans-**5a**. The chemical shifts in trans-**5a** and **8a** are very close, indicating that the phosphines in the two complexes are in similar environments. On the basis of the

(22) Jain, C. L.; Mundley, P. N.; Kumar, Y.; Sethi, P. D. *J. Indian Chem. Soc.* **1989**, *66*, 431−434.
(23) Li, C. S.; Jou, D. C.; Cheng, C. H. *Organometallics* **1993**, *12*, 3945−3954.
(24) Liu, S.; Lucas, C. R.; Newlands, M. J.; Charland, J.-P. *Inorg. Chem.* **1990**, *29*, 4380−4385.
(25) Lucas, C. R.; Liu, S.; Newlands, M. J.; Gabe, E. J. *Can. J. Chem.* **1990**, *68*, 1357−1363.
(26) Latos-Grazynski, L.; Lisowski, J.; Chmielewski, P.; Grzeszczuk, M.; Olmstead, M. M.; Balch, A. L. *Inorg. Chem.* **1994**, *33*, 192−197.
(27) Dean, J. A. *Lange's Handbook of Chemistry*; 15th ed.; McGraw-Hill: New York, 1999.
(28) Bondi, A. *J. Phys. Chem.* **1964**, *68*, 441−451.
(29) Bucknor, S. M.; Draganjac, M.; Rauchfuss, T. B.; Ruffing, C. J.; Fultz, W. C.; Rheingold, A. L. *J. Am. Chem. Soc.* **1984**, *106*, 5379−5381.
(30) Draganjac, M.; Rauchfuss, T. B.; Rheingold, A. L. *Proc. Arkansas Acad. Sci.* **1992**, *46*, 36−38.
(31) Van Stein, G. C.; Van Koten, G.; Blank, F.; Taylor, L. C.; Vrieze, K.; Spek, A. L.; Duisenberg, A. J. M.; Schreurs, A. M. M.; Kojic-Prodic, B.; Brevard, C. *Inorg. Chim. Acta* **1985**, *98*, 107−120.
(32) Goodrich, J. D.; Nickias, P. N.; Selegue, J. P. *Inorg. Chem.* **1987**, *26*, 3424−3426.
(33) Constable, E. C.; Henney, R. P. G.; Tocher, D. A. *J. Chem. Soc., Chem. Commun.* **1989**, 913−914.
(34) Latos-Grazynski, L.; Lisowski, J.; Olmstead, M. M.; Balch, A. L. *Inorg. Chem.* **1989**, *28*, 1183−1188.
(35) Benson, J. W.; Angelici, R. J. *Organometallics* **1992**, *11*, 922−927.
(36) Draganjac, M.; Ruffing, C. J.; Rauchfuss, T. B. *Organometallics* **1985**, *4*, 1909−1911.
(37) Alvarez, M.; Lugan, N.; Mathieu, R. *Inorg. Chem.* **1993**, *32*, 5652−5657.
(38) Latos-Grazynski, L.; Olmstead, M. M.; Balch, A. L. *Inorg. Chem.* **1989**, *28*, 4065−4066.
(39) Deeming, A. J.; Shinhmar, M. K.; Arce, A. J.; Sanctis, Y. D. *J. Chem. Soc., Dalton Trans.* **1999**, 1153−1159.
(40) Hanton, L. R.; Turnbull, J. M.; Richardson, C.; Robinson, W. T. *Chem. Commun.* **2000**, 2465−2466.
(41) Angelici, R. J. *Bull. Soc. Chim. Belg.* **1995**, *104*, 265−282.
(42) Angelici, R. J. *NATO Sci. Ser., Ser. 3* **1998**, *60*, 89−127.
(43) Rauchfuss, T. B. *Prog. Inorg. Chem.* **1991**, *39*, 259−329.
(44) Harris, S. *Polyhedron* **1997**, *16*, 3219−3233.
(45) Bak, B.; Christensen, D.; Hansen-Nygaard, L.; Rastrup-Andersen, J. *J. Mol. Spectrosc.* **1961**, *7*, 58−63.
(46) Choi, M. G.; Angelici, R. J. *J. Am. Chem. Soc.* **1989**, *111*, 8753−8754.
(47) Cotton, F. A.; Wilkinson, G. *Advanced Inorganic Chemistry*; John Wiley & Sons: New York, 1988.

spectroscopic data, we conclude that in the reaction of **5a** with isocyanide the coordinated thiophene is displaced from the Pd.

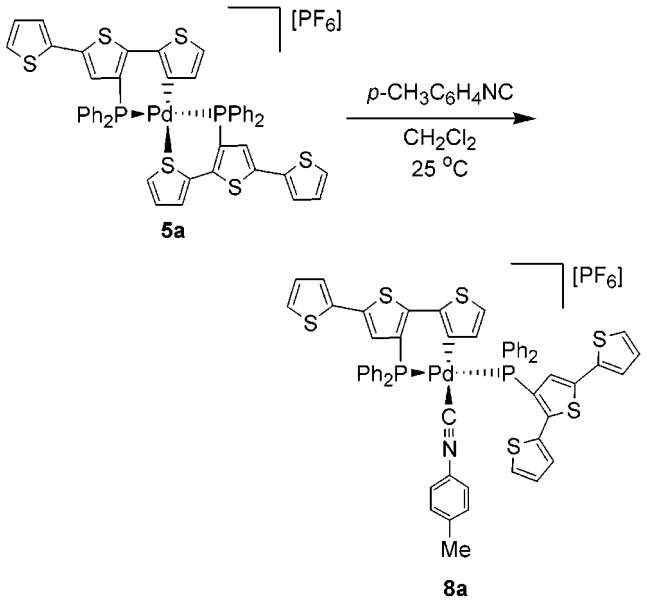

Although **5a** exists as a cis/trans mixture, only one isomer of **8a** is detected by ^{31}P NMR. It is possible that the incoming isocyanide reacts more readily with the trans isomer of **5a**, yielding only **8a**. Another possibility is that the displacement reaction occurs via a trigonal intermediate, in which the structural strain observed in the structure of **5c** is removed. In **5c**, the Pd(II) center lies in an unfavorable geometry deviating from planarity (Figure 1). Upon coordination of isocyanide, displacement of the coordinated thiophene causes one of the dppterth ligands to become monodentate, yielding a complex containing one chelating and two monodentate ligands. This should allow the resulting complex to achieve a more favorable square planar geometry, similar to that of bis(phosphine) complexes **4a**,**b**, where the phosphines are trans, therefore yielding **8a** as the trans isomer only.

Complexes **5b**,**c** also react in a similar fashion with isocyanides to yield products in which the isocyanide is bound via the terminal carbon. For instance, when **5b** was treated with tolyl isocyanide, the product contains a new band at 2191 cm^{-1} in the IR region, characteristic of a C-coordinated isocyanide.

Cyclic Voltammetry of Ligands and Complexes. The cyclic voltammograms (CVs) of compounds **1a**−**c** and **2** contain one irreversible oxidation wave (Table 2) with peak potentials close to that measured for terthiophene (E_p = +1.05 V).[48] The peak oxidation potential of **1a** to **1c** decreases from +1.30 to +1.05 V, because of the addition of the electron donating methyl groups. No reduction wave was observed between 0 and −1.5 V for any of the compounds. Compound **2** has the lowest oxidation potential of all the terthienyl-based compounds reported here, possibly because of the stabilizing influence of the phosphine group on the resulting cation.

None of these phosphinoterthiophene compounds electropolymerized by sweeping the potential repeatedly past the oxidation wave, as evidenced by the absence of film growth on the electrode. For **1b**,**c** and **2**, this result is due in part to the lack of two free α-positions on the oligothiophene necessary for polymerization. In all the compounds, electropolymerization may also be prevented by the nucleophilicity of the free phosphine toward the radical cation formed on the oligothiophene upon oxidation. This is likely the reason **1a** does not electropolymerize, despite two free α-positions and a low oxidation potential.

(48) Diaz, A. F.; Crowley, J.; Bargon, J.; Gardini, G. P.; Torrance, J. B. *J. Electroanal. Chem. Interfacial Electrochem.* **1981**, *121*, 355−361.

Table 2. Cyclic Voltammetry Data

complex	$E_{p,ox}$,[a] ±0.01 V	$E_{p,red}$,[a] ±0.01 V
1a	+1.30	
1b	+1.18	
1c	+1.05	
2	+0.92	
3a[b]	+1.20	−1.31
3b	+1.10 (sh), +1.13	−1.42
3c	+0.91,[c,d] +0.97,[c,d] +1.35	−1.22
4a	+1.27, +1.53	−1.24
4b	+1.34, +1.52	−1.43
4c	+1.07,[c,d] +1.15,[c,d] +1.47	−1.30
5a	+1.31	−1.32
5b	+1.18, 1.39	−1.07
5c	+1.05,[c] +1.42, +1.73	−1.11
6	+1.24, +1.49, +2.03	

[a] Volts vs SCE, Pt working electrode, CH_2Cl_2 containing 0.1 M [(n-Bu)$_4$N]PF$_6$, 20 °C. [b] Reference.[14] [c] $E_{1/2}$. [d] Resolved via semiderivative.[49]

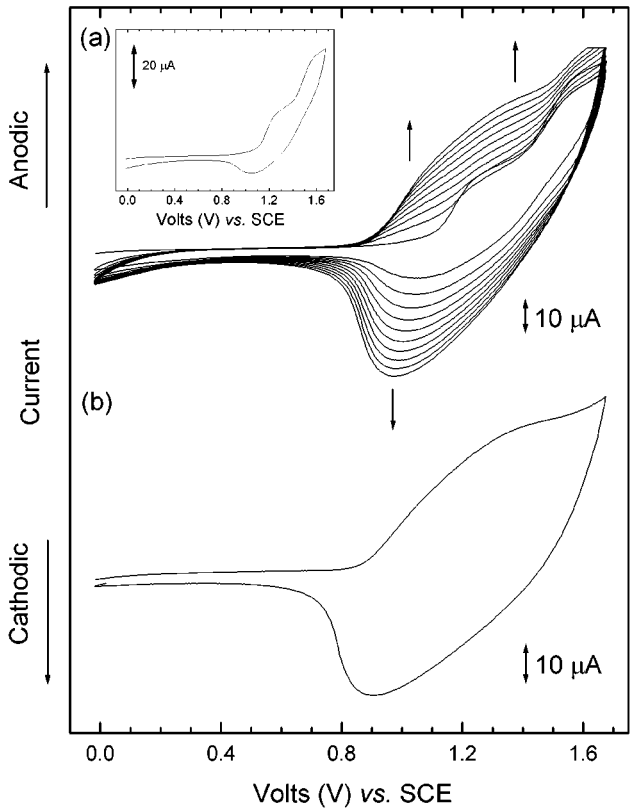

Figure 3. Cyclic voltammetry of **4a** in CH_2Cl_2 containing 0.1 M [(n-Bu)$_4$N]PF$_6$, scan rate = 200 mV/s. (a) Multiple scans from 0 to +1.70 V for **4a**. Inset: first scan of **4a**. (b) Scan of a film of poly-**4a** on a gold electrode.

The cyclic voltammetry of the Pd complexes was carried out in CH_2Cl_2 containing 0.1 M [(n-Bu)$_4$N]PF$_6$, and the data are summarized in Table 2. The CVs of **3a**, **4a**, and **5a** show an oxidation wave near +1.3 V versus SCE and, in the case of **4a**, a second oxidation at +1.53 V (Figure 3a, inset). For **5a**, two overlapping reduction features are visible on the reverse scan (Figure 4a, 1st scan), possibly because of reduction of oligomers of different lengths formed upon scanning past the oxidation wave. The CVs of the complexes containing **1b** all contain two oxidation waves (Table 2). For complex **3b**, these waves are

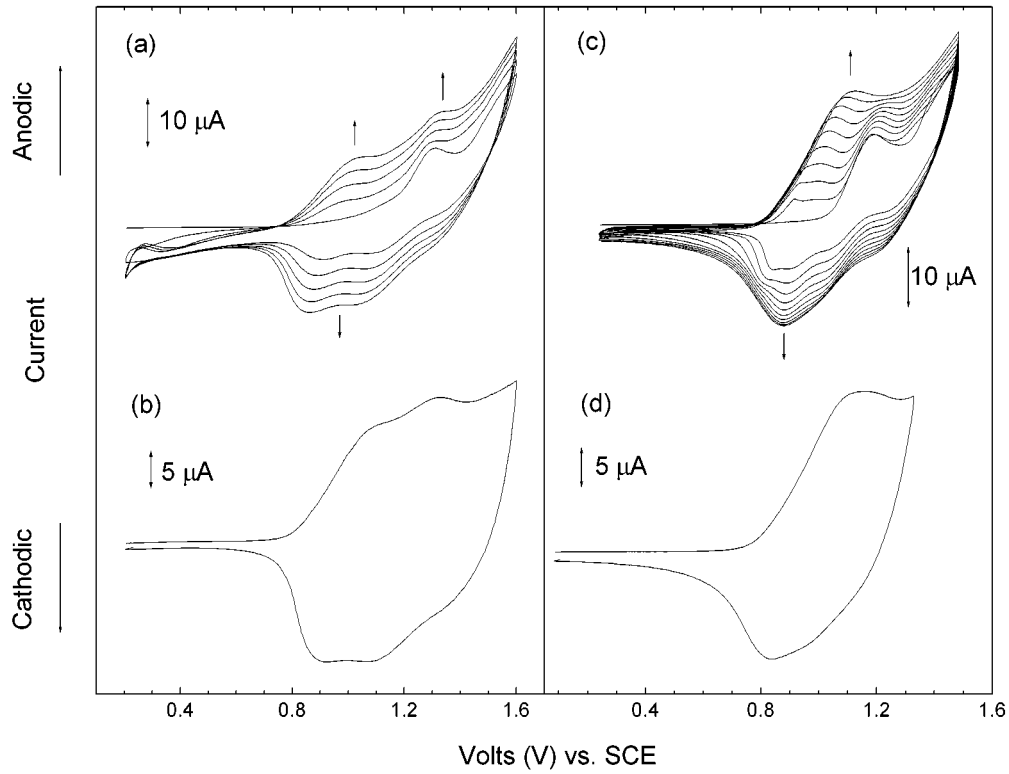

Figure 4. Cyclic voltammetry of **5a** and **5b** in CH_2Cl_2 containing 0.1 M [$(n$-Bu)$_4$N]PF_6, scan rate = 200 mV/s. (a) Multiple scans from +0.20 to +1.60 V for **5a**. (b) Scan of a film of poly-**5a** on a gold electrode. (c) Multiple scans from +0.25 to +1.50 V for **5b**. (d) Scan of a film of poly-**5b** on a gold electrode.

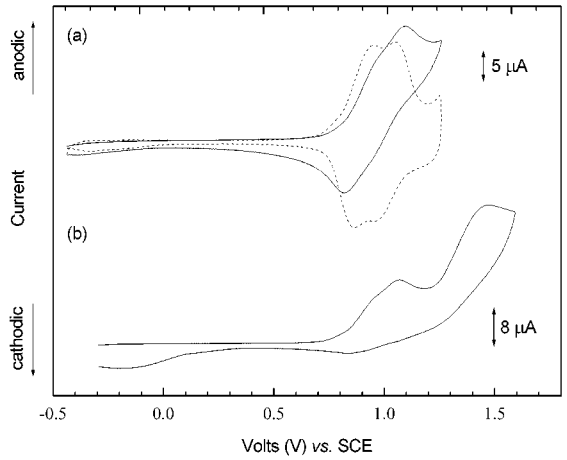

Figure 5. Cyclic voltammetry of **4c** in CH_2Cl_2 containing 0.1 M [$(n$-Bu)$_4$N]PF_6, scan rate = 200 mV/s. (a) Scan from −0.30 to +1.20 V (solid) and semiderivative (dashed). (b) Scan from −0.30 to +1.60 V.

irreversible, while for **4b** the lower potential wave has an associated reduction feature on the reverse scan at +0.88 V. In the case of **5b**, the lower of the two oxidation waves has an associated reduction wave which overlaps with a wave that appears at +0.93 V because of the reduction of longer oligomers (Figure 4c, 1st scan).

The CVs of compounds **3c**, **4c**, and **5c** all contain several redox waves (Table 2). For complexes **3c** and **4c**, the CV contains two overlapping waves near 1 V (shown for **4c** in Figure 5). The waves are reversible if the potential is kept under +1.20 V and were resolved by taking the semiderivative of the CVs, which yield symmetric peaks with a flat baseline.[49] The redox wave for **5c** at +1.05 V becomes irreversible when the potential is scanned past the second oxidation wave (+1.42 V). A third oxidation wave at higher potential is also consistently observed in the CVs of all three complexes containing **1c**. In these complexes, the lowest potential waves are due to oxidation of the Me_2-dppterth ligands.

The number of electrons n involved in the oxidation waves for **4c** and **5c** was determined by adding an internal standard (*cis*-[$RuCl_2$(dmpe)$_2$], dmpe = bis(dimethylphosphino)ethane) to the solution. This standard was chosen because the $Ru^{II/III}$ redox couple is removed from the oxidation peaks of the Pd complexes. The semiderivatives of the voltammograms of these solutions were fitted according to the procedure of Toman and Brown,[49] and the resulting peak heights are then proportional to n^2. For **4c**, the ratio of the peak heights for each of the two resolved oxidation waves to the Ru wave is 0.80; for **5c**, the ratio of the height of the single oxidation wave to the Ru wave is 0.75 (after correcting for concentration differences between the standard and compound). The ratios are both less than unity, consistent with the larger diffusion coefficient expected for the smaller Ru complex. Assuming similar diffusion coefficients for **4c** and **5c**, the similarity between these two ratios shows that the overlapping waves in **4c** are due to two one-electron oxidations, and the single wave in **5c** is due to a one-electron oxidation. The semiderivative peak widths at half-height, which are inversely proportional to n, are also close to those measured for *cis*-[$RuCl_2$(dmpe)$_2$], confirming this conclusion.

Blocking of the α-positions of terthienyl derivatives with methyl groups results in reversible oxidation waves, because the resulting radical cations do not polymerize.[50,51] In **3c** and **4c**, the two terthienyl groups are identical, and the observed splitting in the oxidation waves indicates that there is some

(49) Toman, J. J.; Brown, S. D. *Anal. Chem.* **1981**, *53*, 1497−1504.

(50) Hill, M. G.; Mann, K. R.; Miller, L. L.; Penneau, J. F. *J. Am. Chem. Soc.* **1992**, *114*, 2728−2730.

(51) Hill, M. G.; Penneau, J. R.; Zinger, B.; Mann, K. R.; Miller, L. L. *Chem. Mater.* **1992**, *4*, 1106−1113.

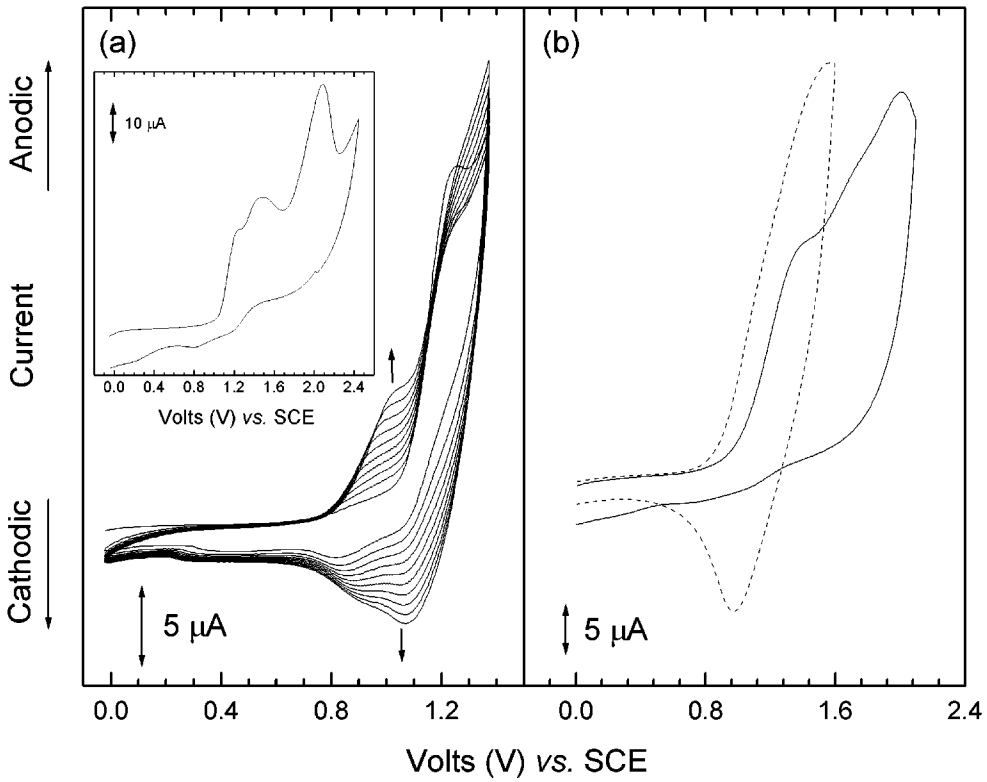

Figure 6. Cyclic voltammetry of **6** in CH_2Cl_2 containing 0.1 M $[(n\text{-}Bu)_4N]PF_6$, scan rate = 200 mV/s. (a) Multiple scans from 0 to +1.40 V for **6**. Inset: first scan of **6**. (b) First scan (dashed) between 0 and +1.60 V and second scan (solid) between 0 and +2.10 V of a film of poly-**6** on a gold electrode.

interaction between the two redox groups. In metal complexes, observation of such splitting has been interpreted as an indication of charge delocalization across the bridge on the electrochemical time scale.[52] In the case of **3c** and **4c**, the splitting is small, suggesting that the interaction is weak. In **5c**, the two terthienyl groups are not identical, and only one of the two is reversibly oxidized at +1.05 V, while the second group is irreversibly oxidized at a higher potential (≥1.4 V). From these results, we can conclude that the interaction between the two terthienyl groups is largest in **5c** (causing the oxidation potential of the second terthienyl group to be shifted well positive of the first), as expected on the basis of the bidentate coordination of both ligands to the Pd in this complex.

The CVs of all the palladium complexes containing **1a**−**c** show one irreversible reduction wave between −1.0 and −1.5 V versus SCE (Table 2). This wave is assigned to a Pd-based reduction process, as **1a**−**c** do not exhibit any reduction waves between 0 and −1.5 V.

Electropolymerization of Pd Complexes. All three Pd complexes containing dppterth electropolymerize when solutions of these monomers are scanned repeatedly over their whole oxidation range. Compound **3a** was previously electropolymerized to form a purple film that is conductive (10^{-3} S cm^{-1}) when oxidized.[14] Electropolymerization of complex **4a** gives a red film of poly-**4a** on the electrode surface, with a concomitant increase in current in the CV (Figure 3a). The CV of the resulting film shows a broad redox feature between +0.7 and +1.6 V (Figure 3b), similar to that observed for poly-**3a** and for other polythiophene derivatives.[14,53] The maximum conductivity of oxidized poly-**4a** is 3×10^{-4} S cm^{-1}, determined in situ by deposition of the film on interdigitated Pt microelectrodes.[54] Similarly, electropolymerization of **5a** (Figure 4a) gave red films (reduced) with a conductivity of 10^{-4} S cm^{-1} when oxidized. The CV of a film of poly-**5a** (Figure 4b) is similar to that observed for poly-**3a** and poly-**4a**.

In contrast, none of the Pd complexes containing Me_2-dppterth (**3c**, **4c**, and **5c**) could be electropolymerized, as evidenced by the absence of film formation on the electrode surface during oxidative cycling. This is not unexpected, because all four α-positions of the terthienyl group in these complexes are blocked by methyl groups, which are known to inhibit thiophene polymerization.[50,51]

In complexes containing Me-dppterth, only two out of four terthienyl α-positions are blocked by methyl groups; nonetheless, all attempts to electropolymerize compound **3b** only resulted in the formation of thin, insulating films on the surface of the electrode. For **4b**, the first few scans showed some increase in current; however, no material was observed on the electrode surface. Variation of the sweep limits and scan rate also did not result in electropolymerization, and any material that eventually formed was either insulating or very poorly conductive. On the other hand, compound **5b** did successfully electropolymerize (Figure 4c) to form orange conductive films, and a CV of this film is shown in Figure 4d.

The cyclic voltammogram of compound **6** contains three oxidation waves and two reduction features on the reverse scan (Figure 6). The lower potential reverse wave is likely due to the reduction of oligomeric species deposited on the electrode after oxidation of the complex. Compound **6** was electropolymerized in a mixture of CH_2Cl_2 and $ClCH_2CH_2Cl$ (1/1 v/v) because of the relative insolubility of this complex in neat CH_2Cl_2. Films of poly-**6** are red when reduced and turn green-black

(52) Barlow, S.; O'Hare, D. *Chem. Rev.* **1997**, *97*, 637−669.
(53) Roncali, J. *Chem. Rev.* **1992**, *92*, 711−738.
(54) Kittlesen, G. P.; White, H. S.; Wrighton, M. S. *J. Am. Chem. Soc.* **1984**, *106*, 7389−7396.

Table 3. EDX Elemental Ratios for the Electropolymerized Materials and Monomers

species	elemental ratio Pd/S	Pd/P	Pd/Cl
poly-**4a**[a]	1.93 ± 0.16	0.66 ± 0.05	1.37 ± 0.11
4[b]	1.58 ± 0.03	0.49 ± 0.02	0.64 ± 0.03
poly-**5a**[c]	1.45 ± 0.02	0.80 ± 0.02	
5a[b]	1.50 ± 0.08	0.65 ± 0.02	
poly-**5b**[c]	1.44 ± 0.15	0.70 ± 0.05	
5b[b]	1.51 ± 0.01	0.65 ± 0.01	
poly-**6**[c]	1.23 ± 0.08	0.55 ± 0.04	0.58 ± 0.01
6[b]	1.31 ± 0.02	0.52 ± 0.01	0.55 ± 0.02

[a] Thin film on indium tin oxide (ITO)/glass. [b]Powder on carbon tape, carbon coated. [c]Thin film on Au.

upon oxidation. The CV of the film shows two oxidation features (Figure 6b). If the potential is scanned only to +1.60 V, a partially reversible redox wave is observed, but when the potential is scanned to +2.10 V, a second oxidation feature is visible and no reduction waves are observed on the reverse scan. This loss of reversibility indicates that poly-**6** is not stable under strongly oxidizing conditions.

All the electropolymerized films were characterized by EDX analysis and the elemental ratios compared to those for the corresponding monomers (Table 3). For all the films except poly-**4a**, the Pd/S ratios measured in the films match those of their monomers within experimental error. The deviation observed for poly-**4a** suggests that side reactions occur during electropolymerization of this species, resulting in anomously high metal content in the film. The Pd/P ratios in the films are comparable to those measured for the monomers, although some excess P is present in the electropolymerized films because of the presence of residual PF_6^-. Further support for the metal complexes remaining intact upon polymerization is provided by the similarity in reactivity between the polymer films and the monomers (vide infra). Attempts to characterize the electropolymerized materials by mass spectrometry were inconclusive because of their instability under MALDI-TOF conditions. Efforts to characterize the Pd monomers using this method, as well as via other mass spectrometric techniques including FAB and EI, were also not fruitful; the parent ions were not observed although fragments due to the ligands were observed in most cases.

Reactivity of the Electropolymerized Films with Isocyanides. The reactivity of poly-**5a** and poly-**5b** films toward isocyanides parallels that of their respective monomers **5a**,**b**. Exposure of films of poly-**5a**,**b** to solutions of *t*-BuNC in hexanes at 25 °C resulted in rapid reaction. The surface reflectance IR spectrum of a film of poly-**5a** after exposure shows a new band at 2219 cm^{-1} due to the CN stretch of an isocyanide coordinated via the terminal carbon. The IR spectrum of **8a** contains a CN stretch of comparable energy. Similarly, when a film of poly-**5b** is exposed to *tert*-butyl isocyanide in hexanes, a new band at 2224 cm^{-1} appears in the surface reflectance IR spectrum of the film, comparable to the CN stretch observed for complex **5b** treated with tolyl isocyanide (2191 cm^{-1}).

In a similar fashion, a film of poly-**3a** was reacted with *t*-BuNC in hexanes, and a new, strong band at 2208 cm^{-1} appeared in the IR spectrum.[14] The film remained insoluble in hexanes after reaction but became highly soluble in CH_2Cl_2. This was attributed to the cleavage of the dichloro bridges in poly-**3a** yielding oligomers with solubilizing *t*-Bu groups added to their backbones.

An increase in the solubility of poly-**5a** and poly-**5b** was also observed after treatment with isocyanides, comparable to that seen for poly-**3a**. When poly-**5a** is reacted with a solution of *p*-tolylisocyanide, the coordinated thiophene is displaced from the metal, leaving the rest of the palladium coordination intact. This results in the addition of one solubilizing group per metal center causing the observed increase in solubility. Unlike the product of the reaction of poly-**3a** with isocyanides, the chains in poly-**5a** and poly-**5b** are not expected to cleave to smaller fragments upon reaction with isocyanide, because the metal remains coordinated to the two dppterth ligands via the phosphine groups, even after displacement of the thiophene.

Table 4. UV−Visible Spectroscopic Data[a]

compound	UV−vis λ_{max}, nm (ϵ, $M^{-1}cm^{-1}$) complex	polymer[e]
1a[b]	254 (2.08×10^4), 354 (1.77×10^4)	
1b	252 (3.42×10^4), 282 (sh) (2.57×10^4), 364 (2.63×10^4)	
1c	254 (2.33×10^4), 362 (2.15×10^4)	
2	248 (1.67×10^4), 376 (3.16×10^4)	
3a[c]	288 (sh) (3.84×10^4), 388 (6.64×10^4)	522 (br)
3b	292 (sh) (3.07×10^4), 346 (3.19×10^4), 396 (4.21×10^4)	
3c	388 (3.25×10^4), 400 (4.59×10^4)	
4a	260 (sh) (3.32×10^5), 348 (5.07×10^5)	442 (br)
4b	264 (sh) (6.72×10^4), 348 (1.02×10^5)	
4c	272 (sh) (4.86×10^4), 354 (6.50×10^4)	
5a	330 (2.43×10^5),[d] 380 (2.09×10^5)[d]	454 (br)
5b	338 (2.27×10^4),[d] 393 (1.04×10^4)[d]	422
5c	268 (sh) (6.47×10^4), 338 (5.32×10^4),[d] 380 (4.62×10^4)[d]	
6	258 (sh) (1.33×10^5), 374 (2.94×10^5)	431
7b	242 (4.64×10^4), 316 (1.28×10^4), 378 (1.17×10^4),[d] 422 (9.46×10^3)[d]	
8a	252 (sh) (9.48×10^4), 352 (4.46×10^4)	

[a] In CH_2Cl_2. [b]Reference.[12] [c]Reference.[14] [d]Overlapping bands. [e] Reduced film on an ITO/glass electrode.

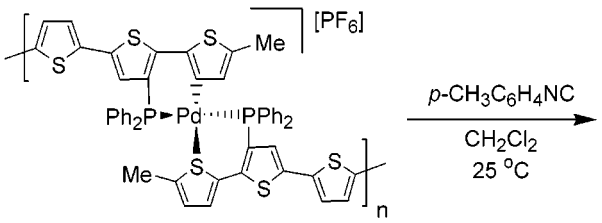

poly-**5b**

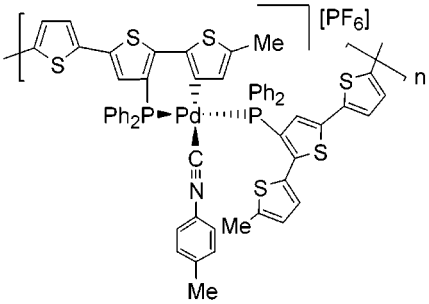

UV−Visible Spectroscopy of 1−6. The UV−vis spectral data for complexes **1**−**6** are shown in Table 4. The spectra of **1a**−**c** and **2** all have absorption bands with a maximum absorbance between 354 and 376 nm, similar to λ_{max} for the $\pi-\pi^*$ transition of terthiophene (351 nm).[55] The spectra of complexes **3a**−**c** contain several absorption bands in the UV tailing into the visible region. All the bands are assigned to ligand-based $\pi-\pi^*$ transitions, by comparison with the UV−

(55) DiCesare, N.; Belletete, M.; Marrano, C.; Leclerc, M.; Durocher, G. *J. Phys. Chem. A* **1999**, *103*, 795−802.

vis spectra of dppterth ligands **1a**−**c** and Ru complexes containing dppterth such as $[RuCl_2(dppterth)_2]$.[12] The low energy bands for **3a**−**c** (388, 396, and 400 nm) are red-shifted from the corresponding bands in **1a**−**c** and follow the same trend observed in the series **1a**−**c**.

The spectra of the bis(phosphine) complexes **4a**−**c** are very similar to each other and contain two bands, corresponding to those observed for the ligands **1a**−**c**. The higher energy bands are slightly red-shifted in the complexes with respect to the corresponding bands in the ligands, while the lower energy bands in **4a**−**c** are blue-shifted both relative to the ligands **1a**−**c** and to the dimetallic complexes **3a**−**c**. A similar blue shift with respect to dppterth was also observed in the ruthenium monocarbonyl complexes *cis*- and *trans*-$[RuCl_2(CO)(dppm)(dppterth$-*P*)].[12] In **4a**−**c**, the blue-shift is likely due to a small electron withdrawing effect by the palladium from the ligands.

Complexes **5a**−**c** show a broad absorption consisting of two overlapping bands with maxima near 340 and 380 nm for all three complexes. These bands are also attributed to ligand-based $\pi-\pi^*$ transitions and are red-shifted both from the parent complexes **4a**−**c** and from the dppterth ligands **1a**−**c**. The red shift is likely due to chelation by the ligands in a bidentate fashion, imposing a rigid conformation on the terthienyl groups. The lower energy band in **5a**−**c** is comparable to the lower band observed both in the dimetallic Pd complexes **3a**−**c** and in the ruthenium complexes in which dppterth is P,S-coordinated such as $[RuCl_2(dppterth$-$P,S)_2]$ and *cis*- and *trans*-$[RuCl_2(dppm)(dppterth$-$P,S)]$.[12] When complex **3b** is reacted with *p*-$CH_3C_6H_4$-NC, the UV−vis spectrum of the resulting mononuclear complex **7b** contains a higher energy band at 316 nm and two lower energy bands at 378 and 422 nm, all of which are assigned to $\pi-\pi^*$ ligand-based transitions.

The spectrum of **8a** contains two bands, both of them blue-shifted relative to parent complex **5a**. Similar behavior was observed when compound **5b** was treated with tolyl isocyanide. A corresponding blue shift also occurs when the ruthenium complexes *cis*- and *trans*-$[RuCl_2(dppm)(dppterth$-$P,S)]$ are treated with CO to give *cis*- and *trans*-$[RuCl_2(CO)(dppm)(dppterth$-*P*)]. The blue shift is therefore likely due to removal of the imposed rigidity in the terthienyl moiety when the ligand becomes monodentate. The absorption band of **8a** is also slightly blue-shifted compared to dppterth, probably because the palladium center is somewhat electron withdrawing. In the spectrum of **6**, two bands are observed, nearly equal in energy to the bands observed for 5dppterth, and are assigned to ligand-based $\pi-\pi^*$ transitions. In complex **6**, coordination of the phosphinoterthiophene ligand via the phosphine does not appear to induce a large perturbation in the electronic structure of the terthienyl group.

UV−Visible Spectroscopy of the Electropolymerized Materials. The spectrum of neutral poly-**4a** shows a broad absorbance at $\lambda_{max} = 442$ nm which shifts to 766 nm upon oxidation. The spectra of neutral poly-**5a** and poly-**5b** contain broadened bands with λ_{max} at 454 and 422 nm, respectively. The band maxima for poly-**4a** and poly-**5a** are red-shifted from those of their corresponding monomers; however, they are also blue-shifted with respect to that of poly-**3a** (522 nm).[14] This is consistent with these materials being composed of oligomers with longer conjugation lengths than their corresponding monomers, but with shorter conjugation than in poly-**3a**. The absorption maximum of neutral poly-**6** is at 431 nm. In poly-**5b** and poly-**6**, the absorption maxima are comparable to that of sexithiophene (432 nm),[56] which is reasonable because these materials are expected to consist predominantly of sexithiophene units linking metal bis(phosphine) groups.

Upon reaction of a poly-**3a** film with *t*-BuNC or PhNC, the absorption band red-shifts to $\lambda_{max} = 528$ nm (*t*-BuNC) and 542 nm for (PhNC).[14] Similarly, the absorption maxima of poly-**5a** and poly-**5b** films treated with *t*-BuNC shift to $\lambda_{max} = 462$ nm and $\lambda_{max} = 434$ nm, respectively. These shifts are indicative of the electronic effect on the backbone caused by the reaction at the pendant metal, and the differences in λ_{max} observed for reactions with two similar isonitriles with poly-**3a** indicate how sensitive the electronic structure of the conjugated backbone is to the ligands at the Pd center.

Discussion

The solid-state structures of **5c**, **3a**,[14] *cis*-$[RuCl_2(dppm)(dppterth$-$P,S)]$,[12] and $[RuCl_2(CO)(dppterth)_2]$[12] all demonstrate that coordination of dppterth via the phosphine alone has little influence on the structure of the terthienyl moiety relative to that of terthiophene. When the dppterth ligands are chelated in a bidentate fashion to the metal, via either the sulfur or C3, the deformations in bond lengths and angles are greater in the coordinated thiophene ring. However, only minor structural deformations are observed in the two remaining rings of the terthienyl moiety. These observations suggest that significant electronic effects (resulting in structural deformations) due to metal centers linked to a polythiophene backbone will occur only when a thiophene ring along the backbone is directly bound to the metal via a sulfur or carbon atom. It is important to note, however, that the extended conjugation that exists along polythiophene chains means that disruption of a single ring in the backbone is sufficient to cause extensive perturbations to the overall electronic properties of the polymer.

Thiophene oligomers polymerize mainly by C−C coupling at the α-(2-) positions.[53] Therefore, it is likely that the obtained films consist primarily of α,α-coupled material, a proposal which is strongly supported by the lack of polymerization observed with the complexes containing **1c**, in which the methyl substituents prevent α,α-coupling.

The materials described in this paper may be divided into two classes on the basis of their structures. In the first class, comprising poly-**5b** and poly-**6**, α,α-coupling results in materials in which the backbone includes the metal centers. In poly-**6**, a linear backbone consisting of phosphine-terminated sexithiophene units linked via metal−dichloro moieties is expected to result from α,α-coupling. Poly-**5b** would form structures in which the methyl-terminated sexithiophene groups are cross-linked via Pd coordinated to phosphorus, sulfur, and carbon atoms. The UV−visible absorption spectra of both materials is similar to that of sexithiophene, supporting the conclusion that the oligothienyl groups in these materials are composed of six-ring units.

In these materials, conductivity results from (a) delocalization of charge along the main chains (including the metal), (b) π-stacking of the oligothiophene units, or (c) a combination of both effects. A conducting copolymer composed of quaterthiophene linked by saturated polyester chains has been reported by Miller et al.,[57] and in this polymer, conductivity only occurs via π-stacks formed with oxidized quaterthiophenes, because delocalization of polarons or bipolarons along the backbone is impossible because of the long saturated linkers between the conjugated moieties.

(56) Van Pham, C.; Burkhardt, A.; Shabana, R.; Cunningham, D. D.; Mark, H. B.; Zimmer, H. *Phosphorus, Sulfur Silicon Relat. Elem.* **1989**, *46*, 153−168.

(57) Hong, Y.; Miller, L. L. *Chem. Mater.* **1995**, *7*, 1999−2000.

The structures of poly-**5b** and of a hypothetical poly-**4b** would be very similar except for the coordination at the palladium center. In **4b**, the oligothienyl units are linked to the metal only via the phosphine groups. On the other hand, in **5b**, the oligothienyl group is linked to the metal not only via the phosphine ligands but also via Pd−C and Pd−S bonds. While complex **5b** electropolymerizes, compound **4b** only yields insulating films upon electrochemical oxidation. Because of the similarities in the structures of the two monomers, this intriguing difference can best be accounted for by examining the CVs of **4c** and **5c** (vide supra). These indicate that the degree of interaction across the metal is larger in **5c**, suggesting that conductivity in poly-**5b** may have a significant contribution from delocalization through the metal. In **4b**, π-stacking alone with a diminished contribution from delocalization across the metal must be insufficient to support the growth of conductive films. Poly-**6** also forms readily by electropolymerization, despite a similar coordination at the metal to **4b**. Here, steric factors also play a role, perhaps allowing better overlap between the conjugated oligothienyl segments than in **4b**, and allowing conductivity via π-stacking to occur.

The second class of materials includes poly-**3a**, poly-**4a**, and poly-**5a**. In these materials, the geometry of the precursor complexes suggests that highly branched species in which oligo- or polythiophene chains are cross-linked by Pd groups will form. Conductivity may arise by delocalization strictly along the conjugated thiophene backbone, as well as via the pathways described above for the first class. In poly-**3a**, conductivity must result primarily from delocalization along the longer polythiophene chains and chain−chain interactions by π-stacking rather than through the Pd−dichloro bridges. The fact that **3b** does not electropolymerize, combined with the small degree of electrochemical interaction across the metal bridge in **3c**, supports this conclusion. The UV−vis absorbance spectrum of poly-**3a**, which is similar to that of other polythiophene derivatives,[58] also demonstrates that the Pd centers have a relatively minor influence on the electronic properties of the material.

Conclusions

The complexes described in this paper allow the electronic interactions in π-conjugated materials containing pendant metal centers to be probed. The electrochemical results for **3c**, **4c**, and **5c** demonstrate that the largest degree of interaction between the dimethylterthienyl groups is seen in **5c** where the metal is both P,C- and P,S-coordinated. In the monomers that have free α-positions, polymerization is observed to occur when the resulting materials have sufficient conductivity to sustain film growth. In the case of **5a** and **5b**, the conductivity appears to involve a contribution from cross-metal delocalization. In **3b** and **4b**, poor delocalization across the metal and poor $\pi-\pi$ overlap between oligothienyl groups prevent electropolymerization because of low conductivity of the resulting films. The observed conductivity in poly-**3a** results primarily from charge delocalization along the extended polythiophene chains and π-stacking rather than through the metal bridges in this material. In poly-**5a** and poly-**5b**, the backbone acts as a hemilabile ligand on the Pd center, remaining coordinated even after displacement of the thienyl moiety. However, even when the material is reacted with a strong σ-donor such as an isocyanide, only small changes in the UV−vis absorption of the film are observed. These results suggest that metal centers that have larger electronic interactions with the polymer backbone may be needed in order to increase the response obtained upon modifying the ligand environment at the metal.

Experimental Section

General. All the reactions were performed using standard Schlenk techniques with dry solvents under nitrogen. Tolyl isocyanide,[59] 3′-diphenylphosphino-2,2′:5′2″-terthiophene (dppterth) (**1a**),[12] and [Pd_2-(μ-Cl_2)(dppterth-*P*,C^3)$_2$] (**3a**)[14] were all prepared according to literature procedures. All other reagents were purchased from either Strem Chemicals or Aldrich and used as received. ^{1}H and ^{31}P NMR experiments were performed on either a Bruker AC-200E or a Bruker AV-300 spectrometer, and spectra were referenced to residual solvent (^{1}H) or external 85% H_3PO_4 (^{31}P). Electronic absorption spectra were obtained on a UNICAM UV2 UV−vis spectrometer. Infrared spectra were obtained on a Bomem MB-series spectrometer on methylene chloride solutions, potassium bromide pellets, or cesium iodide pellets. Surface reflectance IR experiments were performed using a Pike Technologies VeeMax specular reflectance accessory mounted in the Bomem spectrometer. All the surface IR spectra were taken with an incident angle of 45°. Electrochemical measurements were conducted on a Pine AFCBP1 bipotentiostat using a Pt disk working electrode, Pt coil wire counter electrode, and a silver wire reference electrode. An internal reference (decamethylferrocene) was added to correct the measured potentials with respect to saturated calomel electrode (SCE). The supporting electrolyte was 0.1 M [(*n*-Bu)$_4$N]PF_6, which was purified by triple recrystallization from ethanol and dried at 90 °C under vacuum for 3 days. Methylene chloride used in cyclic voltammetry was dried by refluxing over CaH_2. EDX (energy-dispersive X-ray) analysis were performed on a Kevex Quantum light element X-ray detector equipped with a Quartz XOne X-ray analyzer. Note that only a representative synthetic procedure for each group of compounds is given here. Detailed synthetic procedures and complete characterization for the remaining complexes are provided in the Supporting Information.

3′-Diphenylphosphino-5-methyl-2,2′:5′2″-terthiophene (Me-dppterth) (1b). A solution of *n*-butyllithium in hexanes (6.86 mL, 1.6 M, 11.0 mmol) was added dropwise to a solution of 3′-bromo-5-methyl-2,2′:5′,2″-terthiophene (**11**) (3.40 g, 9.97 mmol) in diethyl ether (120 mL) at −15 °C. The mixture was stirred for 1 h at −15 °C and PPh_2Cl (3.31 g, 15.0 mmol) added dropwise. The reaction was then allowed to warm to room temperature and stirred for another 30 min, after which time 1 M HCl was added to quench the reaction. The organic layer was separated, washed with water, and dried over anhydrous $MgSO_4$, and the solvent was removed to yield the crude product, which was purified by chromatography on silica gel with hexanes/methylene chloride (4/1 v/v). The yellow band was collected and the solvent removed to leave a yellow oil. Trituration with a minimum amount of methanol gave **1b** as a yellow powder. Yield: 2.2 g (50%). ^{1}H NMR (200 MHz, $CDCl_3$): δ 7.34 (m, 10H, Ph), 7.15 (m, 1H, Th), 7.05 (m, 1H, Th), 6.95 (m, 2H, Th), 6.65 (m, 1H, Th), 6.58 (s, 1H, Th), 2.46 (s, 3H, CH_3). ^{31}P{^{1}H} NMR (81.015 MHz, $CDCl_3$): δ −24.1 (s). Anal. $C_{25}H_{19}PS_3$ requires C, 67.26; H, 4.26. Found: C, 67.00; H, 4.24%.

[Pd_2(μ-Cl_2)(Me-dppterth-*P*,C^3)$_2$] (3b). A warm solution of Me-dppterth (**1b**) (452 mg, 1.01 mmol) in an ethanol/acetonitrile mixture (40/12 mL) was slowly added at 50 °C to $PdCl_2$ (200 mg, 1.13 mmol) in water (12 mL) and concentrated HCl (0.20 mL). A yellow precipitate immediately formed, and the mixture was stirred for 2 h at 50 °C and filtered warm to yield a yellow powder. The solid was washed with water (2 × 10 mL), ethyl ether (1 × 5 mL), and hexanes (2 × 20 mL) and dried in air. Recrystallization from a chloroform/hexanes mixture yielded an orange solid. Yield: 475 mg (79%). ^{1}H NMR (300 MHz, $CDCl_3$): δ 7.66 (m, 4H, Ph), 7.52−7.24 (m, 14H, Ph and Th), 7.15 (m, 2H, Th), 7.05 (m, 2H, Th), 6.95 (m, 2H, Th), 6.49 (s, 2H, Th), 2.40 and 2.29 (s, 6H, C*H*$_3$). ^{31}P{^{1}H} NMR (121.5 MHz, $CDCl_3$): δ 19.9 (s), 18.7 (s). Anal. $C_{50}H_{36}Cl_2P_2PdS_6$ requires: C, 51.12; H, 3.07. Found: C, 50.83; H, 3.19%.

[$PdCl_2$(dppterth-*P*)$_2$] (4a). To a solution of dppterth (300 mg, 0.69 mmol) dissolved in an ethanol/acetonitrile mixture (20/4 mL) at 50 °C

(58) McCullough, R. D.; Lowe, R. D.; Jayaraman, M.; Anderson, D. L. *J. Org. Chem.* **1993**, *58*, 904−912.

(59) Krapcho, A. P. *J. Org. Chem.* **1962**, *27*, 1089−1090.

was added dropwise a solution of $PdCl_2$ (50.0 mg, 0.28 mmol) in a water/HCl mixture (3 mL, with 0.05 mL concentrated HCl added). Upon addition, a bright lemon-yellow precipitate appeared. After stirring at 50 °C for 1 h, the suspended yellow solid was collected by filtration and washed with water, ether, and hexanes. Recrystallization from methylene chloride/hexanes yielded **4a** as a yellow-orange powder. Yield: 230 mg (79%). ^{1}H NMR (200 MHz, $CDCl_3$): δ 7.69 (m, 4H, *o*-PC_6H_5), 7.48−7.24 (m, 7H, *m,p*-PC_6H_5 and 3-*H*), 7.17−7.08 (m, 2H, 5-*H* and 5″-*H*), 7.02 (dd, 1H, J_{HH} = 3.65 and 1.13 Hz, 3″-*H*), 6.93 (dd, 1H, J_{HH} = 4.91 and 3.65 Hz, 4″-*H*), 6.80 (dd, 1H, J_{HH} = 5.14 and 3.62 Hz, 4-*H*), 6.65 (s, 1H, 4′-*H*). ^{31}P{^{1}H} NMR (81.015 MHz, $CDCl_3$): δ 11.1 (s). Anal. $C_{48}H_{34}Cl_2P_2S_6Pd$ requires: C, 55.31; H, 3.26. Found: C, 55.57; H, 3.32%.

[Pd(dppterth-*P,C*^{3})(dppterth-*P,S*^{1})][PF_6] (5a). To a suspension of **4a** (200 mg, 0.19 mmol) in acetone (40 mL) was slowly added an excess of $AgBF_4$ (84.0 mg, 0.42 mmol) in acetone (40 mL, sparged with nitrogen) at 25 °C. After stirring for 18 h under nitrogen at 25 °C, the mixture was filtered through Celite, and the red filtrate was concentrated to $^1/_{10}$ of the initial volume and added slowly to an aqueous solution of NH_4PF_6 (620 mg, 3.80 mmol) in water (50 mL). The resulting orange slurry was stirred at 25 °C for 30 min, the solid collected by filtration and washed with water (100 mL), diethyl ether (5 mL), and hexanes (50 mL). Slow recrystallization from chloroform/diethyl ether yielded complex **5a** as red crystals. Yield: 180 mg (84%). ^{1}H NMR (200 MHz, $CDCl_3$): δ 7.60−7.40 (m, 21H, Ph and Th), 7.27 (m, 1H, Th), 7.19−7.13 (m, 2H, Th), 7.07−7.00 (m, 3H, Th), 6.96−6.89 (m, 1H, Th), 6.79 (m, 1H, Th), 6.67−6.58 (m, 2H, Th), 6.20 (m, 1H, Th), 6.16−6.10 (m, 1H, Th). ^{31}P NMR (81.015 MHz, $CDCl_3$): δ 25.12 (d, J_{PP} = 19.3 Hz, cis P), 15.7 (d, J_{PP} = 394 Hz, 2P, trans P), 3.8 (d, J_{PP} = 394 Hz, 2P, trans P), 1.9 (d, J_{PP} = 19.3 Hz, cis P), −144.3 (sept, J_{PF} = 713 Hz, 1P, PF_6). Anal. $C_{48}H_{33}F_6P_3S_6Pd$ requires: C, 51.69; H, 2.96. Found: C, 51.19; H, 3.23%.

[PdCl(*p*-$CH_3C_6H_4NC$)(Me-dppterth-*P,C*^{3})] (7b). To a suspension of **3b** (200 mg, 0.19 mmol) in CH_2Cl_2 (7 mL) under N_2 at 25 °C was added *p*-$CH_3C_6H_4NC$ (45.0 mg, 0.38 mmol). After 5 min, the solid was completely dissolved, and the solution was stirred for an additional 20 min, after which time the mixture was concentrated to 2−3 mL under vacuum, and hexanes were added to precipitate a yellow powder. The crude solid was recrystallized from methylene chloride/hexanes to yield pure **7b**. Yield: 202 mg (75%). ^{1}H NMR (200 MHz, $CDCl_3$): δ 7.73−7.53 (m, 4H, *o*-PC_6H_5), 7.50−7.29 (m, *m,p*-PC_6H_5), 7.15 (m, 1H, Th), 7.10−6.90 (m, 5H, Th and C_6H_4NC), 6.72 (m, 2H, C_6H_4NC), 6.53 (m, 1H, Th), 2.41 (s, 3H, Th−CH_3), 2.31 (s, 3H, $CH_3C_6H_4NC$). ^{31}P{^{1}H} NMR (81.015 MHz, $CDCl_3$): δ 17.5 (s). IR (CH_2Cl_2): $\nu_{N\equiv C}$ = 2193 cm^{-1}. Anal. $C_{33}H_{25}ClNPPdS_3$ requires: C, 56.26; H, 3.55; N, 1.99. Found: C, 56.57; H, 3.78; N, 2.00%.

[Pd(*p*-$CH_3C_6H_4NC$)(dppterth)$_2$][PF_6] (8a). To a solution of **5a** (40.0 mg, 0.04 mmol) in CH_2Cl_2 (4 mL) under N_2 at 25 °C was added *p*-$CH_3C_6H_4NC$ (4.19 mg, 0.04 mmol). The solution was stirred for 1.5 h after which time the mixture was concentrated to ∼0.5 mL under vacuum, and hexanes were added to precipitate a yellow powder. The crude solid was recrystallized from methylene chloride/hexanes to yield pure **8a**. Yield: 31 mg (68%). ^{1}H NMR (300 MHz, $CDCl_3$): δ 7.60−7.42 (m, 18H), 7.35−7.30 (m, 2H), 7.22−6.98 (m, 12H), 6.71 (s, 1H), 6.62 (s, 1H), 6.38 (m, 2H), 6.27 (m, 1H), 2.31 (s, 3H, CH_3). ^{31}P{^{1}H} NMR (121.5 MHz, $CDCl_3$): δ 17.5 (d, J_{PP} = 388 Hz, 1P, trans P), 6.4 (d, J_{PP} = 388 Hz, 1P, trans P), −144.3 (sept, J_{PF} = 713 Hz, 1P, PF_6). IR (KBr): $\nu_{N\equiv C}$ = 2194 cm^{-1}. Anal. $C_{56}H_{40}F_6NP_3PdS_6$ requires: C, 54.57; H, 3.25; N, 1.14. Found: C, 54.29; H, 3.29; N, 1.09%.

Table 5. Crystallographic Data for **5c**

	5c·$^2/_3$($CHCl_3$)
formula	$C_{52.67}H_{41.67}Cl_2F_6P_3PdS_6$
mol wt	1251.20
temperature, K	198(2)
crystal system	triclinic
space group	$P\bar{1}$
crystal dimensions (mm^3)	0.25 × 0.15 × 0.03
crystal color	red
a, Å	10.770(1)
b, Å	13.788(1)
c, Å	21.289(4)
α, deg	99.693(5)
β, deg	94.388(5)
γ, deg	112.405(5)
V, Å^3	2846.4(7)
Z	2
reflns collected/unique	17 750/7695 [R_{int} = 0.104]
R1[a], wR2[b] [$I > 3\sigma(I)$]	0.060, 0.072
R1[a], wR2[b] (all data)	0.136, 0.163

[a] $R = \sum||F_o| - |F_c||/\sum|F_o|$. [b] $R_w = \{\sum[w(F_o^2 - F_c^2)^2]/\sum[w(F_o^2)^2]\}^{1/2}$

X-ray Crystallographic Analysis. Suitable crystals of **5c** were grown by slow diffusion of diethyl ether into a solution of the compound in chloroform at ∼15 °C, and data were collected at 198(1) K. Selected crystallographic data for **5c** appear in Table 5. The final unit cell parameters for **5c** were obtained by least-squares on the setting angles for 5689 reflections with 2θ = 4.5−46.1°. All data were processed and corrected for Lorentz and polarization effects and absorption (semiempirical, based on symmetry analysis of redundant data). The structure was solved by direct methods[60] and expanded using Fourier techniques.[61] Final refinements were carried out using teXsan.[62] The complex **5c** crystallizes in space group $P\bar{1}$, with one molecule in the asymmetric unit. The material crystallizes with $CHCl_3$ in the lattice. The solvent molecule site is only partially occupied, with a fraction of approximately $^2/_3$. All non-hydrogen atoms were refined anisotropically, while all hydrogens were placed in calculated positions.

Acknowledgment. We thank the Natural Sciences and Engineering Research Council of Canada for support of this research and Prof. T. M. Swager (M.I.T.) for a generous gift of interdigitated Pt microelectrodes.

Supporting Information Available: Complete synthetic procedures and characterization for **1c**, **2**, **3c**, **4b**,**c**, **5b**,**c**, **6**, **9**−**12** and procedures for electrode preparation and cleaning (pdf). X-ray crystallographic file (CIF) for **5c**. This material is available free of charge via the Internet at http://pubs.acs.org.

JA016465M

(60) Altomare, A.; Burla, M. C.; Camalli, M.; Cascarano, G. L.; Giacovazzo, C.; Guagliardi, A.; Moliterni, A. G. G.; Polidori, G.; Spagna, R. *J. Appl. Crystallogr.* **1999**, *32*, 115−119.

(61) Beurskens, P. T.; Admiraal, G.; Beurskens, G.; Bosman, W. P.; de Gelder, R.; Israel, R.; Smits, J. M. M. *Technical Report of the Crystallography Laboratory*; University of Nijmegen: The Netherlands, 1994.

(62) *Crystal Structure Analysis Package*; The Molecular Structure Corporation: Woodland, TX, 1985 and 1992.